The Pathogenic A2V Mutant Exhibits Distinct Aggregation Kinetics, Metal Site Structure, and Metal Exchange of the Cu2+ -A Complex

Somavarapu, Arun Kumar; Shen, Fei; Teilum, Kaare; Zhang, Jingdong; Mossin, Susanne; Thulstrup, Peter W.; Bjerrum, Morten J.; Tiwari, Manish K.; Szunyogh, Daniel; Søtofte, Peter M.

Total number of authors:
12

Published in:
Chemistry - A European Journal

Link to article, DOI:
10.1002/chem.201703440

Publication date:
2017

Document Version
Peer reviewed version

10.1002/chem.201703440

WILEY-VCH

COMMUNICATION

The Pathogenic A2V Mutant Exhibits Distinct Aggregation Kinetics, Metal Site Structure, and Metal Exchange of the Cu^{2+}-Aβ Complex

Arun K. Somavarapu, Fei Shen, Kaare Teilum, Jingdong Zhang, Susanne Mossin, Peter W. Thulstrup, Morten J. Bjerrum, Manish K. Tiwari, Daniel Szunyogh, Peter M. Søtofte, Kasper P. Kepp and Lars Hemmingsen**

Abstract: A prominent current hypothesis is that impaired metal ion homeostasis may contribute to Alzheimer's Disease (AD). We elucidate the interaction of Cu^{2+} with wild-type (WT) $A\beta_{1-40}$ and the genetic variants A2T and A2V which display increasing pathogenicity as A2T<WT<A2V. Cu^{2+} significantly extends the lag phase in aggregation kinetics, in particular for the pathogenic A2V variant. Additionally, a rapid, initial, low intensity ThT response is observed, possibly reflecting formation of Cu^{2+} induced amorphous aggregates, as supported by AFM and CD spectroscopy, again most notably for the A2V variant. EPR spectroscopy gives pK_a values for transition between two Cu^{2+} coordination geometries (component I and II) of 7.4 (A2T), 7.9 (WT), and 8.4 (A2V), i.e. component I is stabilized at physiological pH in the order A2T<WT<A2V. Similarly, ^{1}H-NMR relaxation exhibits the same trend for the non-coordinating aromatic residues (A2T<WT<A2V), and implies markedly faster inter-peptide Cu^{2+}exchange for the A2V variant than for WT and A2T. We therefore hypothesize that component I of the Cu-Aβ complex is related to pathogenicity, accounting for both the pathogenic nature of the A2V variant and the protective nature of the A2T variant.

More than 30 million people world-wide suffer from Alzheimer's Disease (AD);[1,2] a neurodegenerative disorder that involves loss of cognitive skills and life quality.[3] The biochemical causes of AD remain obscure, current treatments are symptomatic and delay disease progression by only a few months, and more effective treatments of AD thus remain highly prioritized.[4,5] AD is associated with major extracellular plaque deposits and intracellular neurofibrillar tangles.[6] The senile plaques consist of partly modified (N-truncated, oxidized and metal-bound) β-amyloid (Aβ) peptides organized as regular β-sheet-structured fibrils.[7–9] The three major genetic risk factors of familial AD, mutations in the genes APP, PSEN1, and PSEN2 are all related to Aβ strongly implying a role of Aβ in AD, viz. the amyloid hypothesis of AD.[7,9,10]

The broad clinical spectrum of AD[6,11], the facts that >95% of patients do not have a genetic predisposition directly related to Aβ, and that age is the main risk factor of the disease,[12] strongly imply that amyloids are not pathogenic in themselves, but that an age-dependent event must cause the disease.[13] Identifying non-amyloid features that trigger Aβ-driven disease is the motivation of the present work. Specifically, metal ion binding[14–16] and oxidative modifications[17] are characteristic of AD and enforced in the aging human brain,[12,18] and particularly in the hippocampus where AD initiates. [19,20] The upregulation of metal transport proteins in APP/PSEN1 mutant expressing mice[21] and of some metallothioneins[22], and metal-enrichment in senile plaques[15,23,24], suggest that age-enforced metal interactions define the pathogenicity of Aβ.[14,15]

15 sequence variants naturally occurring in humans have been identified in the $A\beta_{1-42}$ region of APP (672−713). Of these, the A2T and A2V mutations are of particular interest, because the A2T variant is protective against cognitive decline in elderly,[25] whereas the A2V variant is pathogenic in homozygous individuals.[26] The first 16 amino acids comprise a high-affinity Cu^{2+} binding site of Aβ.[14,24,27,28], and the carbonyl oxygen or deprotonated backbone amide nitrogen at position 2 have been proposed to be part of the first coordination sphere,[23,24,29] making the A2T and A2V variants particularly interesting in the context of the effect of metal ions in AD. In this work we investigate the binding of Cu^{2+} to Aβ, and the effect on aggregation and structure for three Aβ variants WT, A2V, and A2T.

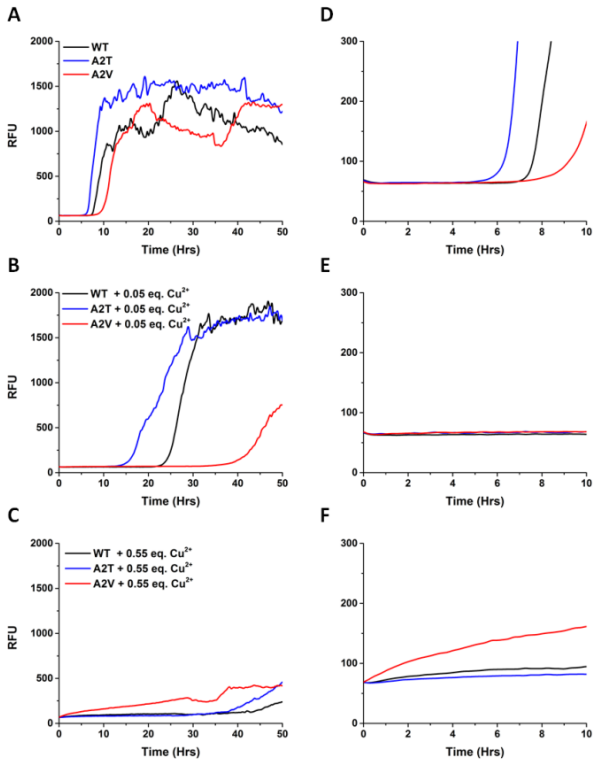

Figure 1. Aggregation kinetics monitored by ThT fluorescence of 20 μM $A\beta_{1-40}$ WT, A2T, and A2V, with A) 0 μM Cu^{2+}, B) 10 μM Cu^{2+}, C) 20 μM Cu^{2+}, and D)−F) are expansions of the first 10 hours time trace of A) – C). All samples were in 43 mM hepes pH 7.4, 86 mM NaCl, 9 μM edta, 12 μM ThT, 37 ºC, and shaking was applied prior to each fluorescence reading. Note that the Cu^{2+} available for binding by Aβ was controlled using edta, that is, this "free" Cu^{2+} is the excess concentration of Cu^{2+} over edta as indicated.

[a] Arun K. Somavarapu, Fei Shen, Prof. Dr. Jingdong Zhang, Prof. Dr. Susanne Mossin, Prof. Dr. K. P. Kepp
DTU Chemistry, Technical University of Denmark
DK 2800 Kongens Lyngby, Denmark
E-mail: kpj@kemi.dtu.dk

[b] Arun K. Somavarapu, Prof. Dr. Peter W. Thulstrup, Prof. Dr. Morten J. Bjerrum, Dr. Manish K. Tiwari, Dr. Daniel Szunyogh, Peter M. Søtofte, and Prof. Dr. Lars Hemmingsen*
Department of Chemistry, University of Copenhagen, Universitetsparken 5, DK-2100 Copenhagen, Denmark
E-mail: lhe@chem.ku.dk

[c] Prof. Dr. Kaare Teilum
Structural Biology and NMR Laboratory and the Linderstrøm-Lang Centre for Protein Science, Department of Biology, University of Copenhagen, Ole Maaløes Vej 5, 2200 Copenhagen N, Denmark

Supporting information for this article is available on the WWW under http://

10.1002/chem.201703440

COMMUNICATION

Aggregation kinetics of all three variants (WT, A2T, and A2V) was elucidated by Thioflavin T (ThT) fluorescence spectroscopy (Figure 1, S1-S5, and Tables S1-S4). In this experiment series we used edta for a dual purpose: 1) In the absence of added Cu^{2+} to bind trace amounts of metal ions, and 2) to control the concentration of free Cu^{2+}: With 9 µM edta and 0, 10, and 20 µM Cu^{2+} in the three series (Figure 1A-C), thus effectively having 0, 1, and 11 µM (or 0, 0.05 and 0.55 eq. with respect to Aβ) free Cu^{2+}. In itself edta does not appear to affect the aggregation kinetics (Figure S6). In the absence of Cu^{2+} only minor differences in the lag time are observed for the three variants, and qualitatively, the expected concentration dependence of the lag time and final ThT fluorescence is observed (Figure 1A, S1 and S5). Day to day and batch to batch variations are presented in Figures S7-S8, indicating that these observations are reproducible. Similar results have previously been obtained[30-33], although with some controversy concerning the order of the lag times for the three variants. We show that there is a batch to batch variation of this order, see Figure S9. Upon addition of Cu^{2+} the lag phase is extended for all three variants in agreement with literature[34–36] (Figure 1, A-C). Most interestingly, the A2V variant is particularly susceptible to the presence of Cu^{2+}, and exhibits a much extended lag phase as compared to the WT and the A2T variant. This may be pathogenically relevant, as the oligomers formed prior to fibrillation are believed to be the pathogenic species[37-39]. Moreover, Cu^{2+} addition gives rise to a rapid low-intensity ThT response, most prominent for the A2V variant (Figure 1F). CD spectroscopic and AFM data, *vide infra*, imply that this early weak ThT response reflects formation of large amorphous aggregates with no well-defined secondary structure, or a spectrum of species with differing secondary structure. Even very low free Cu^{2+} concentration (1 µM free Cu^{2+} / 20 µM Aβ, Figure 1B) significantly increases t_{lag}, and does so particularly for the A2V variant. Thus, with as little as 0.05 eq. Cu^{2+}, all the peptides are affected by the presence of Cu^{2+}. Accordingly, a simple model based on the high affinity of Aβ for Cu^{2+},[40] where Cu^{2+} binds to 5% of the peptides and leaves the remaining 95% unaffected, is not in agreement with the data.

This conclusion is supported by the paramagnetic relaxation enhancement (PRE) recorded in ^{1}H-NMR, where all peptides are affected by the presence of 0.1 eq. Cu^{2+} within a very short time span, *vide infra*. These findings agree with the sub-stoichiometric early Cu^{2+}-induced non-fibrillar aggregation observed for the wild-type Aβ by Pedersen et al.[41] Higher free Cu^{2+} concentrations, yet still at sub-stoichiometric conditions (11 µM free Cu^{2+} / 20 µM Aβ, Figure 1C) further delays the fibrillation. All the observed trends of the ThT experiments for the A2T, WT, and A2V variants of Aβ are qualitatively maintained at low ionic strength (Figure S3), and when no shaking is applied (Figure S4), i.e. these conclusions are robust against such changes in experimental conditions.

AFM data (Figure 2 A-C, Figure S10 A-C) recorded for samples that were dropcasted on mica sheets and dried for 4 hours, display no significant indication of aggregation as compared to the background (Figure S13). This observation corroborates the ThT fluorescence data, indicating no significant aggregation at early times in the absence of Cu^{2+}, and is further supported by the CD spectroscopic data (Figure 3A), indicating no significant presence of ordered secondary structure, *vide infra*. After two weeks fibrils appear for both the WT and A2T variant, while the A2V variant has assembled into aggregates with no clear presence of fibrils (Figure 2G-I, Figure S11 A-C). After three weeks (Figure 2 M-O, Figure S12 A-C), the WT and A2T variant remain fibrillary (Figure 2M and 2N), and while the A2V variant exhibits clear fibril-like structures, the morphology and length differ significantly from the other two variants (Figure 2O, Figure S12C). The fibrils are considerably longer, the height distribution significantly shifted towards larger values, and there appear to be "beads" deposited along the fibrils, possibly reflecting amorphous aggregates associating with the fibrils. Addition of Cu^{2+}, controlling the free Cu^{2+} concentration using edta in the same manner as in the ThT fluorescence, *vide supra*, gives rise to formation of large aggregates for all three variants (Figure 2 D-F, J-L, P-R) already after 4 hours, and overall these large aggregates persist for the duration of the experiment series. The results are in agreement with literature data for the WT.[42]

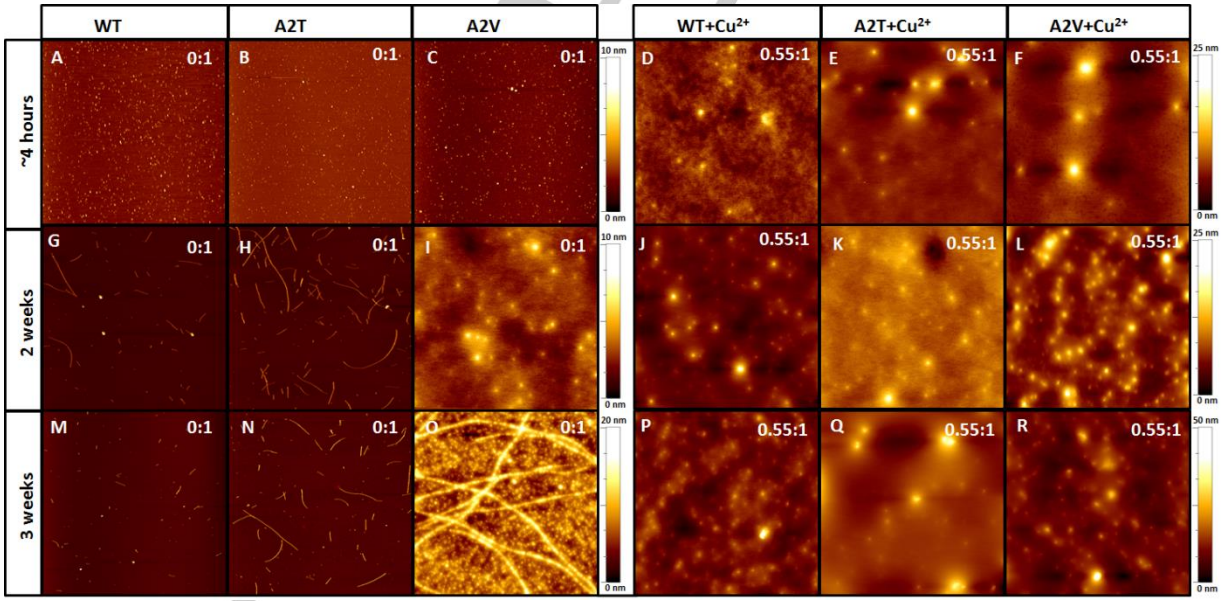

Figure 2. AFM images (5 × 5 µm^2, tapping mode) of $A\beta_{1-40}$ variants at different metal:peptide ratios (0:1 or 0.55:1) and 20 µM Aβ, 4 mM hepes pH 7.4, 9 µM edta and 37°C, without shaking, and with sample age as indicated. A-C) sample age of ~ 4 hours; D-F) same as A-C in presence of 20 µM Cu^{2+}; G-I) sample age of 2 weeks; J-L) same as G-I in presence of 20 µM Cu^{2+}; M-O) sample age of 3 weeks; P-R) same as M-O in presence of 20 µM Cu^{2+}. Corresponding height distributions are presented in Figures S10-S12.

CD spectroscopic data indicate that initially (Figure 3A) all three variants display signatures of random coil in agreement with

10.1002/chem.201703440

literature,[30,42] and although there are minor changes upon addition of Cu^{2+}, no obvious formation of ordered secondary structure occurs at short time scales (Figure 3C).

Figure 3B and 3D display CD spectra recorded for the end point samples of the ThT time trace (Figure S3, Table S3) without and with Cu^{2+} present, respectively. In the absence of Cu^{2+} the spectra are very similar for WT and A2T, while the A2V variant gives a distinct signal. This is intriguing since all three samples have reached essentially the same final level of ThT response (Figure S3C). The difference cannot originate simply from differences in the concentration of Aβ because the absorption spectra exhibit only minor differences (Figure S14). This indicates that the secondary structure composition of fibrils of A2V differs from that of the other two variants.

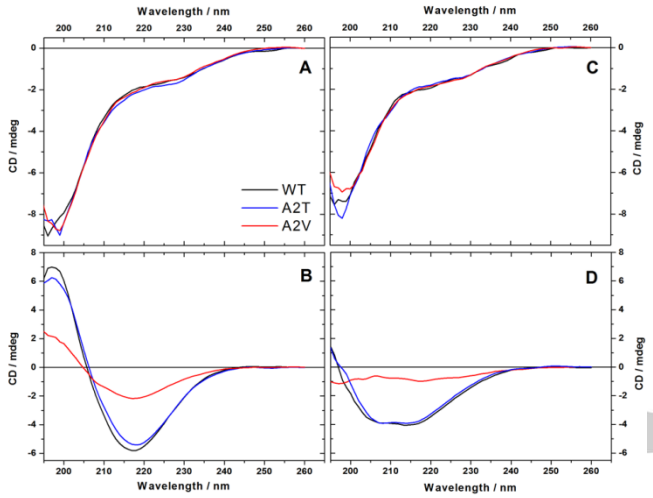

Figure 3. CD spectra recorded immediately after sample preparation, panels A and C, and for end point samples, panels B and D, collected from ThT experiments (Figure S3; note that A2V + Cu^{2+} (panel D) had not formed ThT responsive fibrils at the end point). 20 μM Aβ, 4 mM hepes pH 7.4, 0 μM Cu^{2+} (panels A and B) or 20 μM Cu^{2+} (panels C and D), 9 μM edta and 37 °C.

The CD spectra are typical for antiparallel β-sheet structure. However, these features are clearly reduced for the A2V variant, possibly due to signal cancellation from contributions by less ordered species (Table S5), in agreement with the distinct morphological properties as probed by AFM. Thus, the CD and AFM data indicate that the A2V variant forms more complex aggregates, encompassing both fibrillar structures and components richer in helix or coil structure, even when the fibrillation has converged towards the final ThT fluorescence. In the presence of Cu^{2+}, interestingly, the A2V variant still displays no well-defined secondary structure after 90 hours in the Cu^{2+}-induced prolonged lag phase (Figure 3D). This implies that the A2V peptides are trapped in Cu^{2+}-induced aggregates with no well-defined or a spectrum of secondary structures prior to fibrillation. The WT and A2T variant have fibrillized (Figure S3D) and display very similar CD spectra indicating well-defined secondary structure (Figure 3D), similar to spectra observed for the WT after eight days by Kirkitadze *et al.*, which were interpreted as indicating increased α-helix character.[43] Based on deconvolution of the CD data, the change induced by Cu^{2+} corresponds to a ~10% lower content of antiparallel β-sheet and an increase in both helix and random coil (~6-7%) content (Table S5).

Paramagnetic relaxation enhancement (R1,PRE) for the aromatic region of the ^{1}H-NMR spectrum for all three $Aβ_{1-16}$ variants is shown in Figure 4A (for ^{1}H-NMR spectra see Figure S15). The observed PRE of the His6, His13, and His14 residues is higher than for the others, reflecting that they are involved in copper coordination in the WT,[23,28] and that this is also the case for the two genetic variants. The PRE for WT and A2T are similar, while for A2V it is significantly higher. The experiments are carried out with only 0.1 eq. Cu^{2+} relative to the peptide, i.e. the rapid relaxation of protons of all the peptides indicates that Cu^{2+} is rapidly exchanged between peptides. To test if this might occur via free Cu^{2+} and be due to weaker Cu^{2+} binding of the A2V variant, potentiometric and fluorometric determination of the K_d for metal ion dissociation was conducted, see Figures S16-S18, Table S6. The results demonstrate only minor (less than a factor of ~3) differences in the K_d values between the A2T, WT, and A2V variants, and therefore the affinity of the peptides for Cu^{2+} is too high for the exchange to occur via free Cu^{2+}.[44] Thus, the PRE experiments reflect Cu^{2+} exchange occurring via transient formation of metal ion bridged dimers or higher oligomers, and this process is apparently significantly faster for the A2V variant than for the WT and A2T variant.

Figure 4. A) Paramagnetic relaxation enhancement (R_1,PRE) for the aromatic

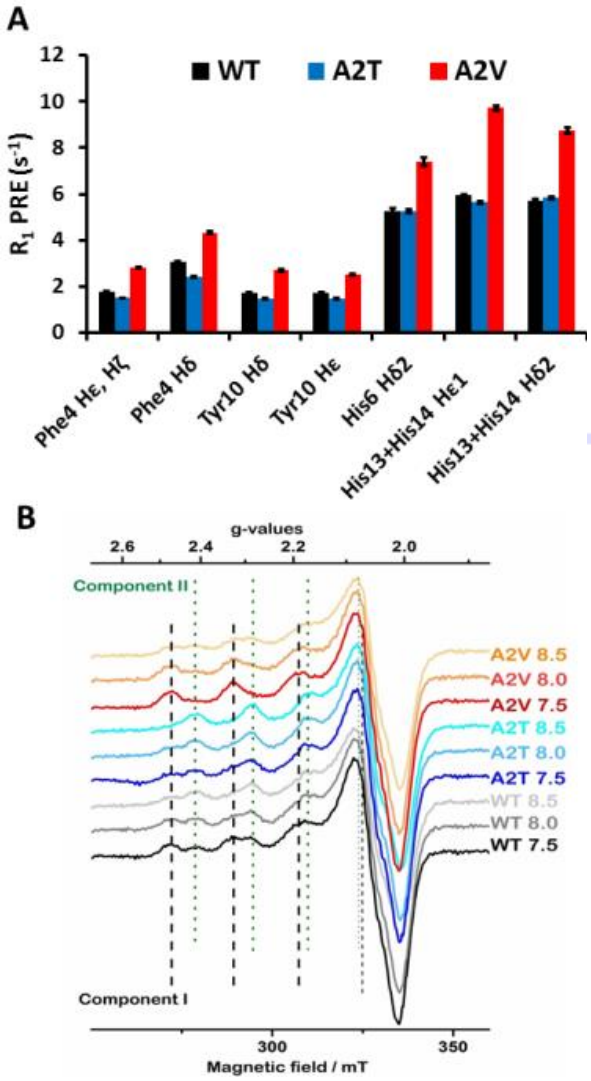

residues in $Aβ_{1-16}$. 300 μM Aβ, 30 μM $CuCl_2$, 60 μM glycine, 150 mM of NaCl, ~10% D_2O and pH 7.4 at 25 °C, no buffer. B) EPR spectra obtained at 77 K for 300 μM Aβ in the presence of 240 μM $CuCl_2$, 10 mM hepes and 110 mM NaCl at pH 7.5, 8.0, and 8.5.

EPR spectra recorded for all three $A\beta_{1-16}$ variants (Figure 4B) reveal the coexistence of two Cu^{2+} coordination geometries. The spin Hamiltonian parameters for component I are $g_{\|} = 2.258$, $g_{\perp} = 2.05$, $A_{\|} = 177 \cdot 10^{-4}$ cm^{-1} and for component II $g_{\|} = 2.230$, $g_{\perp} = 2.05$, $A_{\|} = 157 \cdot 10^{-4}$ cm^{-1} in agreement with literature.[29,45] Despite the fact that the mutations (A2T and A2V) occur near the metal site binding region of the peptide, the parameters of the two sites do not change between variants, but the population differs and depends on pH. The pK_a values for the transition from component I to component II is ~7.4 (A2T), ~7.9 (WT), and ~8.4 (A2V) (Figure S19). Importantly, this feature reflects the trend in clinical pathogenicity (A2T<WT<A2V). While it was shown previously that component I dominates in A2V[45] at physiological pH, this finding becomes more significant in the light of the opposite effect of the protective A2T variant. That is, component I is stabilized as A2T<WT<A2V at physiological pH. Interestingly, the ^{1}H-NMR relaxation rates observed for the Phe4 and Tyr10 protons (Figure 4A) exhibit the same trend (A2T<WT<A2V), suggesting that Cu^{2+} exchange between peptides may occur via component I or a transient structure more readily accessible from component I than from component II. The relative relaxation rates of the His (imidazole) protons show a slightly different pattern (A2T≈WT<A2V), possibly due to a slightly different propensity to coordinate to Cu^{2+}.

Using peptides of increasing clinical pathogenicity (A2T < WT < A2V) we have demonstrated that Cu^{2+} binding site structure and exchange, differs between the variants in a manner that parallels the pathogenicity. We tentatively propose that component I which is stabilized in the A2V variant at physiological pH, is related to pathogenicity. It is conceivable that the preponderance of component I is also the origin of the initial weak ThT response and the delayed fibrillation, observed for the A2V variant in the presence of Cu^{2+}. It is interesting to note that this is in excellent agreement with the increased propensity of the WT Aβ-Cu^{2+} complex to rapidly form aggregates under mildly acidic conditions, where component I is also stabilized.[46] This would imply that the WT protein should exhibit a longer lag time than the A2T variant in the presence of Cu^{2+}, which cannot be concluded unequivocally from the current study. However, other minor differences between WT and the A2T variant aggregation kinetics rate constants might counteract the effect of component I, giving rise to the observed time course of the ThT fluorescence.

Although this work represents only pure *in vitro* chemistry, it is tempting to speculate on the implications for the presumably far more complex molecular speciation occurring during the development of Alzheimer's disease. The correlation between properties of the Aβ-Cu^{2+} complex and pathology of the A2V variant, supports a role of Cu^{2+} in the etiology of AD, and points to component I as a potential molecular culprit. Remarkably, if this hypothesis is correct, it presents a common age-enforced molecular mechanism for the initiation of both sporadic and genetic AD, suggesting a synergistic effect between genetic and chemical effectors in the development of AD, intertwining the etiology of familial (A2V) and sporadic (WT) AD with a central role of Cu^{2+} in both forms of the disease.

Acknowledgements

The Danish Council for Independent Research | Natural sciences (DFF – 1323-00110B), the Danish Council for Independent Research | Technology and Production (DFF – 4005-00082), and the Lundbeck Foundation (R141-2013-13028) are acknowledged for support. We thank the Carlsberg Foundation for funding an upgrade of the EPR equipment at DTU (grant 2012-01-0797).

Keywords: Alzheimer's disease • amyloid beta • aggregation • copper • oligomers • spectroscopy

(1) World Health Organization. *Fact sheet on dementia*; 2015.
(2) Alzheimer's Disease International. *World Alzheimer Report 2015: The Global Impact of Dementia*; 2015.
(3) Kepp, K. P. *Prog. Neurobiol.* **2016**, *143*, 36.
(4) Goedert, M.; Spillantini, M. G. *Science* **2006**, *314*, 777.
(5) Sorrentino, P.; Iuliano, A.; Polverino, A.; Jacini, F.; Sorrentino, G. *FEBS Lett.* **2014**, *588*, 641.
(6) Karantzoulis, S.; Galvin, J. E. *Expert Rev. Neurother.* **2011**, *11*, 1579.
(7) Hardy, J.; Selkoe, D. J. *Science (80-.).* **2002**, *297*, 353.
(8) Masters, C. L.; Selkoe, D. J. *Cold Spring Harb. Perspect. Med.* **2012**, *2*, a006262.
(9) Masters, C. L.; Gajdusek, D. C.; Gibbs, C. J. J. *Brain* **1981**, *104*, 535.
(10) Wolfe, M. S.; Xia, W.; Ostaszewski, B. L.; Diehl, T. S.; Kimberly, W. T.; Selkoe, D. J. *Nature* **1999**, *398*, 513.
(11) Tiwari, M. K.; Kepp, K. P. *Alzheimer's Dement. J. Alzheimer's Assoc.* **2016**, *12*, 184.
(12) Lu, T.; Pan, Y.; Kao, S.-Y.; Li, C.; Kohane, I.; Chan, J.; Yankner, B. A. *Nature* **2004**, *429*, 883.
(13) Zhu, X.; Raina, A. K.; Perry, G.; Smith, M. A. *Lancet. Neurol.* **2004**, *3*, 219.
(14) Kepp, K. P. *Chem. Rev.* **2012**, *112*, 5193.
(15) Bush, A. I. *Rev. Lit. Arts Am.* **2013**, *33*, 277.
(16) Kozlowski, H.; Luczkowski, M.; Remelli, M.; Valensin, D. *Coord. Chem. Rev.* **2012**, *256*, 2129.
(17) Perry, G.; Cash, A. D.; Smith, M. A. *J. Biomed. Biotechnol.* **2002**, *2*, 120.
(18) Bush, A. I.; Tanzi, R. E. *Neurotherapeutics* **2008**, *5*, 421.
(19) Paoletti, P.; Vergnano, A. M.; Barbour, B.; Casado, M. *Neuroscience* **2009**, *158*, 126.
(20) Frederickson, C. J.; Danscher, G. *Prog. Brain Res.* **1990**, *83*, 71.
(21) Zhang, L.-H.; Wang, X.; Stoltenberg, M.; Danscher, G.; Huang, L.; Wang, Z.-Y. *Brain Res. Bull.* **2008**, *77*, 55.
(22) Hidalgo, J.; Carrasco, J.; Quintana, A.; Molinero, A.; Florit, S.; Giralt, M.; Ortega-Aznar, A. *Exp. Biol. Med.* **2006**, 1450.
(23) Faller, P.; Hureau, C.; La Penna, G. *Acc. Chem. Res.* **2014**, *47*, 2252.
(24) Faller, P.; Hureau, C. *Coord. Chem. Rev.* **2012**, *256*, 2127.
(25) Jonsson, T.; Atwal, J. K.; Steinberg, S.; Snaedal, J.; Jonsson, P. V.; Bjornsson, S.; Stefansson, H.; Sulem, P.; Gudbjartsson, D.; Maloney, J.; Hoyte, K.; Gustafson, A.; Liu, Y.; Lu, Y.; Bhangale, T.; Graham, R. R.; Huttenlocher, J.; Bjornsdottir, G.; Andreassen, O. A.; Jönsson, E. G.; Palotie, A.; Behrens, T. W.; Magnusson, O. T.; Kong, A.; Thorsteinsdottir, U.; Watts, R. J.; Stefansson, K. *Nature* **2012**, *488*, 96.
(26) Di Fede, G.; Catania, M.; Morbin, M.; Rossi, G.; Suardi, S.; Mazzoleni, G.; Merlin, M.; Giovagnoli, A. R.; Prioni, S.; Erbetta, A.; Falcone, C.; Gobbi, M.; Colombo, L.; Bastone, A.; Beeg, M.; Manzoni, C.; Francescucci, B.; Spagnoli, A.; Cantù, L.; Del Favero, E.; Levy, E.; Salmona, M.; Tagliavini, F. *Science* **2009**, *323*, 1473.
(27) Viles, J. H. *Coord. Chem. Rev.* **2012**, *256*, 2271.

(28) Drew, S. C.; Barnham, K. J. *Acc Chem Res* **2011**, *44*, 1146.
(29) Hureau, C. *Coord. Chem. Rev.* **2012**, *256*, 2164.
(30) Murray, B.; Sorci, M.; Rosenthal, J.; Lippens, J.; Isaacson, D.; Das, P.; Fabris, D.; Li, S.; Belfort, G. *Proteins* **2016**, *84*, 488.
(31) Benilova, I.; Gallardo, R.; Ungureanu, A.-A.; Castillo Cano, V.; Snellinx, A.; Ramakers, M.; Bartic, C.; Rousseau, F.; Schymkowitz, J.; De Strooper, B. *J. Biol. Chem.* **2014**, *289*, 30977.
(32) Maloney, J. A.; Bainbridge, T.; Gustafson, A.; Zhang, S.; Kyauk, R.; Steiner, P.; van der Brug, M.; Liu, Y.; Ernst, J. A.; Watts, R. J.; Atwal, J. K. *J. Biol. Chem.* **2014**, *289*, 30990.
(33) Lin, T.-W.; Chang, C.-F.; Chang, Y.-J.; Liao, Y.-H.; Yu, H.-M.; Chen, Y.-R. *PLoS One* **2017**, *12*, e0174561.
(34) Tõugu, V.; Karafin, A.; Zovo, K.; Chung, R. S.; Howells, C.; West, A. K.; Palumaa, P. *J. Neurochem.* **2009**, *110*, 1784.
(35) Mold, M.; Ouro-Gnao, L.; Wieckowski, B. M.; Exley, C. *Sci. Rep.* **2013**, *3*, 1.
(36) Chen, W.-T.; Hong, C.-J.; Lin, Y.-T.; Chang, W.-H.; Huang, H.-T.; Liao, J.-Y.; Chang, Y.-J.; Hsieh, Y.-F.; Cheng, C.-Y.; Liu, H.-C.; Chen, Y.-R.; Cheng, I. H. *PLoS One* **2012**, *7*, e35807.
(37) Ono, K.; Condron, M. M.; Teplow, D. B. *Proc. Natl. Acad. Sci. U. S. A.* **2009**, *106*, 14745.
(38) Walsh, D. M.; Selkoe, D. J. *J. Neurochem.* **2007**, *101*, 1172.
(39) Li, S.; Jin, M.; Koeglsperger, T.; Shepardson, N. E.; Shankar, G. M.; Selkoe, D. J. *J. Neurosci.* **2011**, *31*, 6627.
(40) Alies, B.; Renaglia, E.; Rózga, M.; Bal, W.; Faller, P.; Hureau, C. *Anal. Chem.* **2013**, *85*, 1501.
(41) Pedersen, J. T.; Østergaard, J.; Rozlosnik, N.; Gammelgaard, B.; Heegaard, N. H. H. *J. Biol. Chem.* **2011**, *286*, 26952.
(42) Messa, M.; Colombo, L.; del Favero, E.; Cantu, L.; Stoilova, T.; Cagnotto, A.; Rossi, A.; Morbin, M.; Di Fede, G.; Tagliavini, F.; Salmona, M. *J. Biol. Chem.* **2014**, *289*, 24143.
(43) Kirkitadze, M. D.; Condron, M. M.; Teplow, D. B. *J. Mol. Biol.* **2001**, *312*, 1103.
(44) Pedersen, J. T.; Teilum, K.; Heegaard, N. H. H.; Østergaard, J.; Adolph, H. W.; Hemmingsen, L. *Angew. Chemie - Int. Ed.* **2011**, *50*, 2532.
(45) Drew, S. C.; Masters, C. L.; Barnham, K. J. *PLoS One* **2010**, *5*, e15875.
(46) Pedersen, J. T.; Borg, C. B.; Michaels, T. C. T.; Knowles, T. P. J.; Faller, P.; Teilum, K.; Hemmingsen, L. *ChemBioChem* **2015**, *16*, 1293.

10.1002/chem.201703440

WILEY-VCH

COMMUNICATION

Entry for the Table of Contents

COMMUNICATION

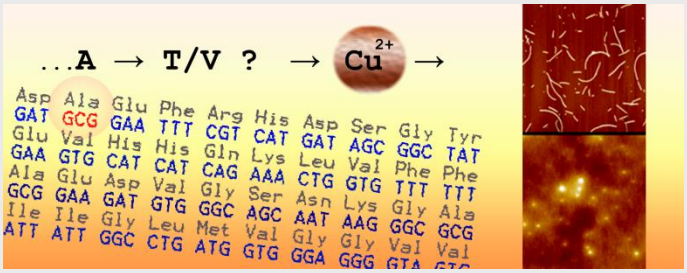

Arun K. Somavarapu, Fei Shen, Kaare Teilum, Jingdong Zhang, Susanne Mossin, Peter W. Thulstrup, Morten J. Bjerrum, Manish K. Tiwari, Daniel Szunyogh, Peter M. Søtofte, Kasper P. Kepp and Lars Hemmingsen**

Page No. 1 – Page No. 4

The Pathogenic A2V Mutant Exhibits Distinct Aggregation Kinetics, Metal Site Structure, and Metal Exchange of the Cu^{2+}-Aβ Complex

The Pathogenic A2V Mutant Exhibits Distinct Aggregation Kinetics, Metal Site Structure, and Metal Exchange of the Cu^{2+}-Aβ Complex

Is component I of the Cu^{2+}-Aβ complex a molecular culprit of Alzheimer's disease?